ARTICLE

Robustness and timing of cellular differentiation through population-based symmetry breaking

Angel Stanoev[1] | **Christian Schröter**[1] | **Aneta Koseska**[1*]

[1]Department of Systemic Cell Biology, Max Planck Institute of Molecular Physiology, Dortmund, Germany

Correspondence
Email:
*aneta.koseska@mpi-dortmund.mpg.de

Although coordinated behavior of multicellular organisms relies on intercellular communication, the dynamical mechanism that underlies symmetry breaking in homogeneous populations, thereby giving rise to heterogeneous cell types remains unclear. In contrast to the prevalent cell-intrinsic view of differentiation where multistability on the single cell level is a necessary pre-requisite, we propose that heterogeneous cellular identities emerge and are maintained cooperatively on a population level. Identifying a generic symmetry breaking mechanism, we demonstrate that robust proportions between differentiated cell types are intrinsic features of this inhomogeneous steady state solution. Critical organization in the vicinity of the symmetry breaking bifurcation on the other hand, suggests that timing of cellular differentiation emerges for growing populations in a self-organized manner. Setting a clear distinction between pre-existing asymmetries and symmetry breaking events, we thus demonstrate that emergent symmetry breaking, in conjunction with organization near criticality necessarily leads to robustness and accuracy during development.

KEYWORDS
symmetry breaking; differentiation; inhomogeneous steady state

Abbreviations: IHSS, inhomogeneous steady state

1 | INTRODUCTION

Symmetry breaking events characterize a transition from an initially homogeneous to a heterogeneous distribution of the constituents within a system, and therefore undoubtedly underlie emergence of biological complexity. These events are generated and the state is maintained on a systems level through self-organized cooperative processes, whose resulting dynamics cannot be deduced from the features of the individual constituents (Zhang and Hiiragi, 2018; Li and Bowerman, 2010; Kauffman, 1993). Even more, the relatively low information content about a system resulting from symmetries implies that information originates at symmetry breaking, and therefore these events are directly linked to emergent computational features. For example, the functional diversification during development arises through symmetry breaking within a homogeneous group of cells, leading to differentiated cell types (Zhang and Hiiragi, 2018; Simon et al., 2018). In this process, not only the specification of distinct cell fates is suitably determined, but also the number distribution of each cell type must be robust against perturbations. Additionally, the onset of the symmetry breaking and thus differentiation must be accurately timed.

The observations that expression of mutually exclusive genetic markers distinguish the differentiated fates among each other and from the multilineage primed state have promoted the hypothesis that multistability on the level of single cells sets the dynamical basis for differentiation (Kauffman, 1969; Andrecut et al., 2011; Wang et al., 2011; Enver et al., 2009). The most common functional motif that accounts for bistability on a single cell level is a two-component genetic toggle-switch (Thomas, 1981; Cherry and Adler, 2000; Snoussi, 1998), whereas addition of self-activating loops (Huang et al., 2007; Bessonnard et al., 2014; Jia et al., 2017) gives rise to a third stable state - the multilineage primed co-expression state. Such single cell multistable circuits have been used to describe the Gata1/PU.1 switch that governs the lineage commitment in multipotent progenitor cells (Huang et al., 2007; Graf and Enver, 2009), the Cdx2/Oct4 switch in the differentiation of the totipotent embryo (Niwa et al., 2005), the T-bet/Gata3 switch in the specification of the T-helper cells (Huang, 2013) as well as the Gata6/Nanog switch in the branching process of inner cell mass (ICM) (Bessonnard et al., 2014; Chickarmane and Peterson, 2008). Generating asymmetries in these systems and thereby adopting a particular fate is typically attributed to stochastic events or cell-to-cell heterogeneities, which are in turn amplified by intercellular signaling to drive the individual cellular states out of the multilineage primed attractor (De Mot et al., 2016). Within such a description however, symmetry breaking does not formally occur, but rather pre-existing inhomogeneities are necessary for lineage commitment to occur. This current single cell input-output view where extracellular signals, which serve as bifurcation parameters, switch the cellular state between co-existing attractors, does not account neither for the robustness in the number distribution of cell types in a population, nor for the timing of the symmetry breaking onset. Moreover, an emergent symmetry breaking mechanisms that generalizes how a population of identical cells gives rise to differentiated cellular identities, while simultaneously accounting for the beginning and robustness of the process is not known.

On the level of tissues and organisms on the other hand, cells do not only unidirectionally process the information from the environment, but continuously modulate the extracellular signals by secreting growth factors or other signaling molecules to communicate their intrinsic dynamical state with the neighboring cells. This in turn redefines the communication signal as a variable rather than a bifurcation parameter, and thus the population of cells must be studied as a joint dynamical system, rather than a collection of individual input-output entities. Using this formalism, we propose a dynamical mechanism where the population of identical cells breaks the symmetry due to cell-to-cell communication, giving rise to a novel heterogeneous dynamical solution that is different than the combinations of the solutions of the isolated cells. In this framework, the intercellular communication initially induces the non-differentiated multilineage primed state from which the differentiated fates emerge upon symmetry breaking. We identified that the transition from homogeneous to a heterogeneous population is governed by a unique bifurcation scenario, resulting in

the formation of an inhomogeneous steady state (IHSS) (Koseska et al., 2013), that reflects the cooperatively occupied differentiated cell fates. Contrary to the current understanding, we not only demonstrate that higher order single-cell multistability does not represent a symmetry breaking mechanism, but it is also not a pre-requisite to account how cellular fates emerge and are maintained. Reliable cell proportions in the differentiated fates are an inherent feature of the symmetry-breaking IHSS solution, whereas parameter organization in its vicinity renders timing of cellular differentiation an emergent property of a growing population of equivalent cells. This population-based symmetry breaking mechanism is generic and applies to systems with diverse gene expression dynamics in isolated single cells, as we use it to describe the differentiation of the ICM state in the case of the mammalian preimplantation embryo.

2 | RESULTS

2.1 | Heterogeneous cellular identities emerge via a population-based inhomogeneous steady state solution

We consider a generic case where the single cell dynamics is governed by a minimal model of a genetic toggle switch, composed of two genes u and v that inhibit each other by repressing transcription from their respective promoters P_u and P_v. We assume here that the growth factor molecules s negatively affect the expression of the switch gene u and their expression is in turn also regulated by the dynamics of the toggle-switch (Fig. 1A, inset). Thus, for intercellular signals that are produced by the cells themselves, the secreted molecules are no longer a parameter, but rather a variable in the system (Eq. (1)). On the level of a single cell, the system is monostable with respect to the expression strength of the promoter P_u, α_u (Fig. 1A). However, the bifurcation analysis even for a minimal population of two identical cells recursively interacting via the secreted signaling molecules revealed multiple different dynamical regimes (Fig. 1B). In a given range of α_u only a single fixed point is stable (Fig. 1B and Fig. 1C, top). This homogeneous steady state (HSS) represents the multilineage primed state, where both u and v are co-expressed. At a critical α_u value, the HSS breaks symmetry via a pitchfork bifurcation: the HSS looses its stability, and a pair of fixed points is stabilized, thereby giving rise to an inhomogeneous steady state (IHSS) (Fig. 1B). The IHSS is a single dynamical solution that has a heterogeneous manifestation: the unstable HSS splits into two symmetric branches that gain stability via saddle-node bifurcations (Koseska et al., 2013), and correspond to a high u-expression state in one cell (u_2) and low u-expression state in the other cells ($u_1 < u_2$), (Fig. 1D). These branches reflect the differentiated cellular identities that emerge from the multilineage primed HSS. These results therefore show that tristability is not a necessary requirement to describe neither the multilineage primed state, nor the differentiated state, but rather cellular fates emerge due to cell-to-cell interactions.

Unlike the independent steady states in a classical bistable system, the two IHSS branches are conjugate to each other. For two coupled cells therefore, a high u-expressing state in one and a low u-expressing state in the other cell always emerge, even when the cells are completely identical based on their parameters (Fig. 1D). In that sense, the IHSS arising via a pitchfork bifurcation is a true symmetry breaking solution, since it inevitably and robustly leads to differentiated cellular identities. Generally, for N globally coupled cells, $N - 1$ different distributions of the cells in the two branches are possible, such that distributions are represented by attractors in phase space (Koseska et al., 2010). For example, for $N = 4$ globally coupled cells, three different IHSS distributions are stable: one cell having high- and 3 having low-expressing u state ($1h3l$), two cells in each branch ($2h2l$) or 3 cells with high and one with low expressing u state ($3h1l$) (Fig. 1E). These distributions are always ordered towards increasing number of cells with high-u expression state for increasing α_u, whereas the branches of the neighbouring distributions overlap in parameter space (Fig. 1E). Thus, it follows that reliable proportions of cells in the differentiated fates are a natural consequence of the IHSS solution. Which proportion will be observed for a specific system only relies on the organization of that system in

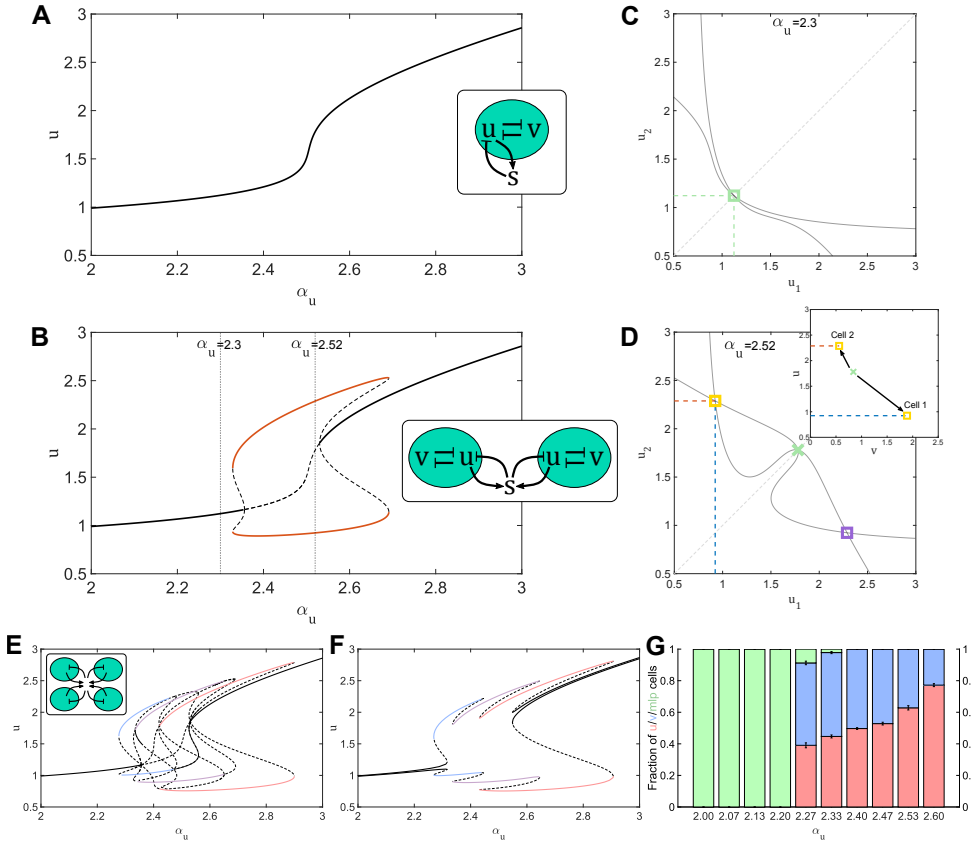

FIGURE 1 Emergence of cellular identities via population-based symmetry breaking. (A) Bifurcation diagram depicting monostable behavior on the level of single cells with respect to changes of promoter strength α_u. Inset: underlying single cell network topology. (B) Bifurcation analysis for two coupled identical cells (inset) reveals emergence of symmetry breaking via a pitchfork bifurcation (PB) and corresponding inhomogeneous steady state (IHSS) solution. Solid lines depict stable steady states: homogeneous steady state (HSS, black) and IHSS (red); Dashed lines - unstable steady states. (C) Phase plane analysis for organization in the HSS ($\alpha_u = 2.3$) depicting the nullclines of the coupled system. (D) Emergence of symmetric heterogeneous states for organization in the IHSS ($\alpha_u = 2.5$). Inset: Manifestation of the IHSS state. Mutually exclusives genetic markers mark the two differentiated states. (E) Bifurcation analysis of a system of globally-coupled $N = 4$ cells. 3 stable IHSS distributions with increasing u+/v+ cell ratios appear sequentially. Blue: 1 cell in the higher, 3 in the lower u-expression state ($1h3l$); Violet: $2h2l$ and Red: $1l3h$. (F) Equivalent bifurcation analysis for non-identical cells (see Methods). Line description as in 1B, and colors as in 1E. (G) u/v cell proportions for increasing α_u. Non-locally coupled population of $N = 32$ cells on a 4×8 grid is considered. Parameters in Methods.

parameter space.

Parameter differences between single cells on the other hand, promote the stability region of the IHSS (Koseska et al., 2009). Bifurcation analysis in the case where cell-to-cell variability in α_u was present (Methods) revealed that each cell is already characterized slightly differently with the HSS. This initial asymmetry in turn promotes the symmetry breaking solution such that the parameter range where neighbouring distributions overlap decreases (Fig. 1F) and subsequently, the robustness of the cell proportions in the two differentiated fates increases. It can be therefore concluded

that the number of cells acquiring specific fates is conserved under cell-to-cell variability. These results demonstrate that several crucial dynamical characteristics emerge for a population-based symmetry-breaking phenomenon: i) the undifferentiated co-expression state directly arises from the cell-to-cell communication and does not require evoking higher-order multistability on the level of a single cell, ii) heterogeneous cellular identities are generated from initially identical cells and are maintained on a population level and iii) reliable proportions of differentiated cells are a direct consequence of the IHSS solution and can be robustly maintained under cell-to-cell variability.

To probe whether reliable population ratios can be achieved for signaling with different communication ranges, we next considered three different cell-cell coupling scenarios: global (all-to-all), local (nearest neighbor) and non-local (nearest and second nearest neighbour) coupling. For non-locally coupled $N = 32$ cells, the proportion of high-u expressing cells progressively increased (Fig. 1G) as predicted by the bifurcation analysis for the globally coupled cells (Fig. 1E). For local coupling however, 50-50% ratio was maintained even for increasing α_u, indicating that regular salt-and-pepper pattern on a 4×8 lattice is always the most probable solution (not shown). This analysis however also showed that for $N = 32$ cells, specifications were observed for α_u values for which in the case of $N = 2$ coupled cells, only the multilineage primed state (the HSS) was stable (compare Fig. 1G and Fig. 1B). This inevitably opens the question how the timing of cellular differentiation is determined.

2.2 | Timing of cellular differentiation as an intrinsic feature of growing populations organized at criticality

It is typically assumed that a change of a bifurcation parameter, such as for example extracellular concentration of signaling molecules s, drives the system through a dynamical transition, thereby relating the onset of differentiation to characteristic reaction rates (De Mot et al., 2016). Considering on one hand that s is not a parameter but a dynamical variable for the system, and on the other hand that the majority of system parameters such as the promoter expression strength in the studied example, are determined by the underlying molecular details and cannot significantly deviate, question has to be posed what triggers the symmetry breaking event during differentiation. The experimental observations that the multilineage primed state is maintained for several cell cycles before differentiation occurs (Saiz et al., 2016) suggests that for $N = 2$ coupled cells, the system is positioned in the HSS, before the pitchfork bifurcation (Fig. 1B). We therefore explore the possibility how cell fate specification from the multilineage primed state occurs for fixed system organization in parameter space.

Since for N globally coupled cells, $N - 1$ IHSS distributions are possible, it can be deduced that the distribution number increases as 2^n with the cell divisions, where n denotes the step in the lineage tree. This inclusion of the new distributions at each cell division event widens the parameter range where the IHSS is stable (compare Fig. 1B with Fig. 1E). Thus, in the parameter region where for $N = 2$ coupled cells only the HSS was stable, for $N \approx 4 - 8$ non-locally coupled cells, stable IHSS branches appeared (Methods), (Fig. 2A). This renders the number of cells and thereby the size of the population as the effective bifurcation parameter that triggers cellular differentiation.

To demonstrate how organization before the α_u-bifurcation point can serve as a timing mechanism that regulates the onset of differentiation, we generated a lineage tree where the population growth is represented in a simplified way: after a given time period T that mimics cell cycle length, all cells divide and the number of cells is doubled. The starting gene expression states of the daughter cells are equal to the final state of the mother cell. Initially, all cells populate the multilineage primed state. As the cell population grows in size and the IHSS distributions appear in the parameter space where the system is positioned, the intrinsic stochasticity of gene expression will be sufficient to induce jump to the coexisting IHSS solution. In this process the majority of the cells populate one of the two IHSS branches of a particular cell type distribution (Fig. 2B). Analysis of the distribution proportions for increasing system size showed approximately

conserved distribution above a certain population size ($N \approx 16$ cells, Fig. 2B, upper panel).

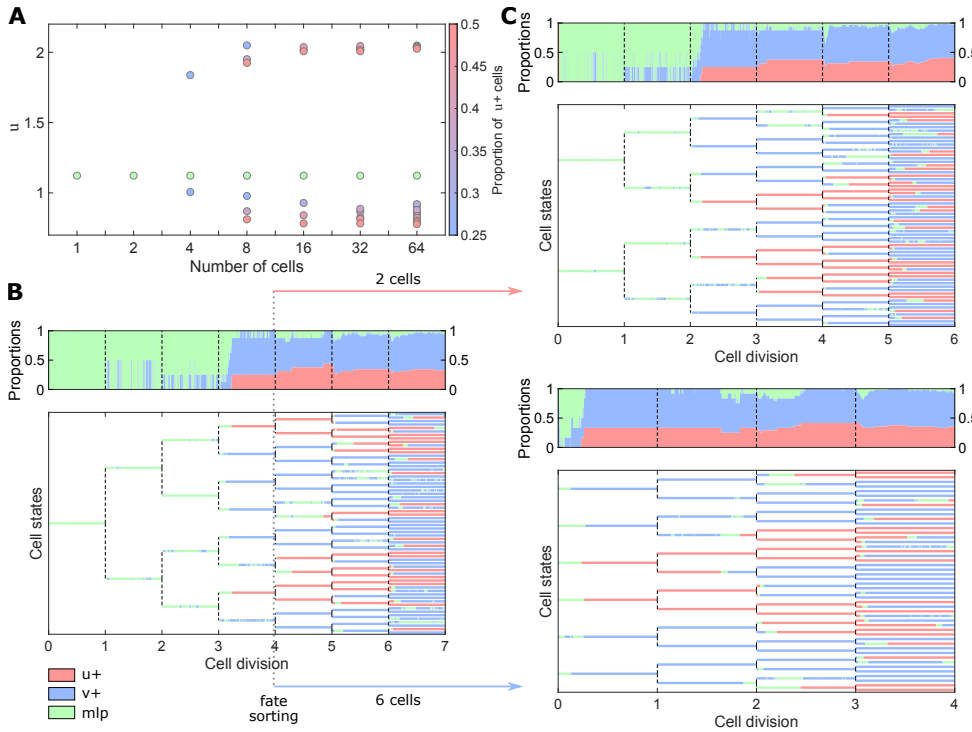

FIGURE 2 Organization near criticality determines timing of differentiation events. (A) Emergence of stable IHSS distributions for increasing cell number N and organization before the pitchfork bifurcation ($\alpha_u = 2.3$). Populating the distinct stable distributions is estimated from multiple stochastic realizations of the system by quantifying the convergence to one of the respective distributions (Methods). Other parameters as in Fig. 1B. (B) Lineage tree demonstrating differentiation from the multilineage primed state as a function of the cell number for systems organization at criticality. Green: cells in the multi lineage primed state; Red: cells with high u–expression state; Blue: cells with low u-expression state (high v-expression state). Upper panel: respective cell type proportions. (C) Lineage trees generated from homogeneous sub-populations of differentiated cells. At $n = 4$th step of the lineage tree ($N = 8$ cells) in Fig. 2B, differentiated cells of identical fates are sorted, and the respective evolution of the sub-systems is followed to generate: (Top) Lineage tree seeded from the $N = 2$ cells that before sorting adopted the high u–expression state ($u+$); (Bottom) Lineage tree seeded from the $N = 6$ cells that initially had adopted the low u–expression state ($v+$). Both upper panels reflect the corresponding cell type proportions.

This mechanism of generating and maintaining heterogeneous cellular identities on a population level we propose here also implies than differentiated fates coexist. We therefore performed a numerical experiment in which cells at $n = 4$th step of the lineage tree ($N = 8$ cells, Fig. 2B) are sorted according to their fates, forming two single-fate sub-populations of different size that can further grow and divide (Fig. 2C). The sub-population of two coupled cells with high u-expression initially reverted to the multilineage primed fate, but after 3 cell cycles ($N = 8$ cells state), both differentiated fates re-emerged (Fig. 2C, top). The other sub-population of $N = 6$ cells with low u-expression on the other hand, initially briefly re-visited the multilineage primed state before both cell types stably re-emerged (Fig. 2C, bottom). The cell type ratios for both sub-populations were quickly stabilized to a fixed value similar to that

of the full system before sorting, and differed among each other $\approx 6\%$. This scaling and regenerating capability of the system is a direct consequence of the conjugacy of the two IHSS branches: dynamically, it is not allowed to populate the upper without populating the lower stable branch of the respective distribution. Thus, even when cells are sorted such that only the cells whose dynamics follows high u-expression state remain, the cell division and thereby the cell-cell communication through which IHSS emerges in a first place will enable the system to recover both cell types with reliable ratios.

2.3 | Reliable proportions of differentiated cells are intrinsic feature of the IHSS solution

To probe the robustness of cell type ratios, we next investigated the effects of variance in the initial conditions, as well as presence of intrinsic noise that is ubiquitous in gene expression. The results are obtained for a population of $N = 32$ non-locally coupled cells and a fixed α_u organization before the symmetry breaking bifurcation as in (Fig. 2B). Neither sampling the single cell initial conditions from distributions with increasing standard deviations nor from distributions where the mean value shifts from high u-expression to high v-expression state (0 to 1), significantly affected the ratio between the two cell types (Fig. 3A,Fig. 3B). The stochastic simulations demonstrated similarly reliable ratios, even for increasing noise intensity (Fig. 3C).

To investigate whether this robustness indeed arises due to the population-induced symmetry breaking and thereby the IHSS solution, we also analyzed if reliable cell proportions can be achieved when considering that cellular identity is an intrinsic feature of single cells. Following this current view of differentiation, tristability on the level of single cells is the necessary requirement to account for the multilineage primed as well as the differentiated fates, whereas intercellular signaling only drives the cells in one of the existing attractors (De Mot et al., 2016). Dynamical systems theory however states that cell-to-cell communication can lead to novel dynamical solutions of the coupled system that are different than those of the isolated cells, indicating that the features of the coupled system cannot be explained with those of single cells (Suzuki et al., 2011; Goto and Kaneko, 2013; Koseska et al., 2007; Ullner et al., 2008). The proposed symmetry breaking mechanism is also a demonstration of this principle. It would be therefore formally correct to exploit the concept of multistability as a basis for differentiation only when this reflects the dynamics of the full communicating system. We therefore generated a paradigmatic multistability model where toggle switch with self-activation leads to tristability on the level of single cells (Jia et al., 2017), but also the dynamics of the coupled system (Eq. (2)) resulted in a tristable behavior (Fig. 3G). In this case, the linage commitment was not robust, and the fate decisions were completely determined by the distributions of initial conditions or the amplitude of the noise intensity. Either all cells remained in the multilineage primed state, or all cells populated a single differentiated state. (Figs. 3D to 3F,Fig. 3H). The pronounced difference in the dynamical behavior of a single cell multistable system and the IHSS lies in the fact that the IHSS is a true symmetry breaking solution. As a consequence of the symmetry breaking phenomenon, the two IHSS branches emerge together and as previously noted, are conjugate to each other, thereby always leading to a fixed number of cells in each of the differentiated fates. On the other hand, when multistability occurs on the level of the coupled system, all of the cells will populate only single attractor, reflecting that it is a solution of the joint dynamical system (Figs. 3G and 3H). The population-based multistability analysis therefore does not support dynamical co-existence of heterogeneous cellular identities in this system. Asymmetrical distributions between the co-existing attractors of a multistable system are only possible when the tristability reflects the dynamics of single cells, in absence of intercellular communication. In this case, differences in the initial expression levels determine the attractor that each cell will occupy (Fig. 3H, gray squares). Thus, neither a transition between a homogeneous, multilineage primed state towards a heterogeneous, differentiated state occurs, nor robustness of the cell type ratios can be accounted for.

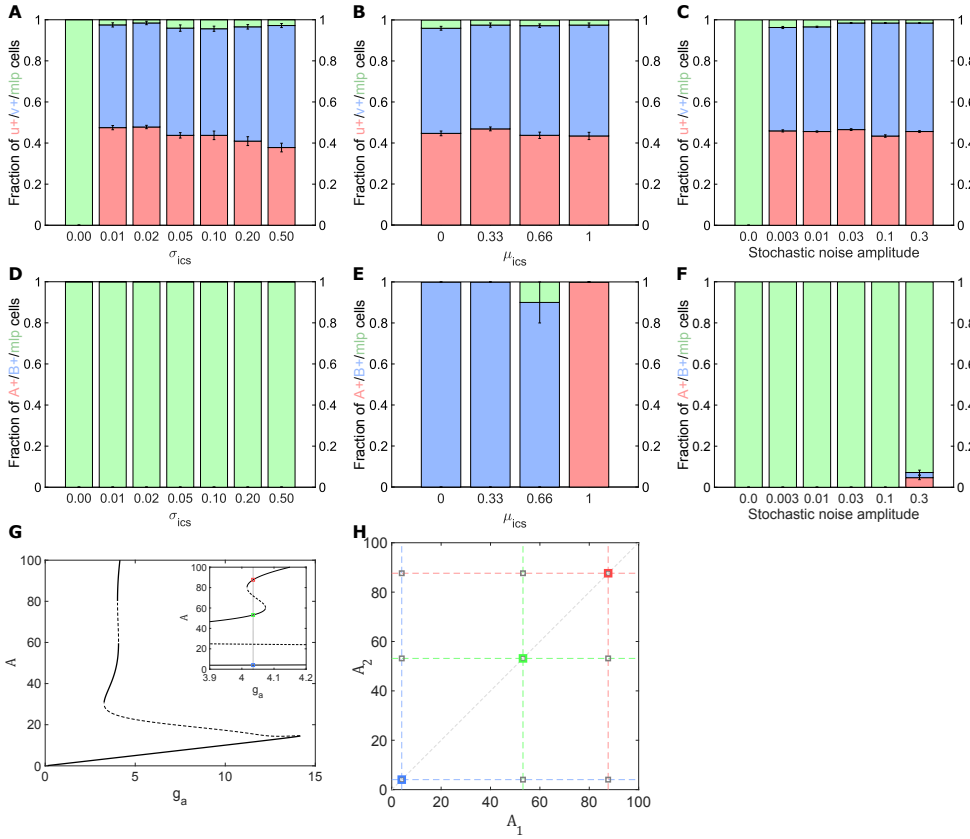

FIGURE 3 Comparison of robustness in cell ratios between symmetry-breaking and pre-existing asymmetry-based mechanisms. Cell type proportions for: (A) gradual increase in the variance of the initial conditions distribution (σ_{ics}); (B) shift in the distribution's mean (μ_{ics}) value from high u-expression to high v-expression state; and (C) increase in the stochastic noise intensity. Average of ten independent numerical realizations for each conditions are shown, estimated for a population of $N = 32$ non-locally coupled cells on an 4×8 grid and organization before the pitchfork bifurcation as in (Fig. 2B). (D-F) Same as in A-C, estimated for $N = 32$ non-locally coupled cells exhibiting tristability on a population level (Eq. (2)). (G) Bifurcation diagram of the System (2) exhibiting tristability on a single as well as population level (inset: zoomed-in tristability region) and (H) Attractor occupancy for both cases. The colored squares represent the three possible solutions of the coupled system, whereas the gray squares determine the possible combinations of single cell solutions.

2.4 | IHSS as a generic mechanism for cellular differentiation: case study of the early embryo

The proposed symmetry breaking solution together with the systems organization before the pitchfork bifurcation uniquely provides a dynamical mechanism of differentiation that simultaneously accounts for the computational features emerging at such self-organization event. These properties can be directly related to the population-based pitchfork bifurcation and are therefore independent of the gene expression dynamics in single cells. We demonstrate this using bistable single-cell behavior, as pervasive during embryogenesis.

During early embryogenesis, Nanog and Gata6 expressions are directly related to differentiated epiblast (Epi) and

primitive endoderm (PrE) fates respectively, whereas their differentiation from the inner cell mass (ICM) cells relies on intercellular interactions involving Erk signaling through Fgf4 communication (Schröter et al., 2015; Bessonnard et al., 2014; Chazaud et al., 2006). The mechanism for ICM differentiation in wild-type embryos has been postulated to be a consequence of tristability on the level of single cells. The heterogeneities in extracellular Fgf4 concentrations that each cell perceives have been determined as crucial to set the switching threshold upon which cells populate one of the remaining stable attractors (De Mot et al., 2016; Bessonnard et al., 2014). This single-cell identity view has been used to explain the occurrence of purely Epi or PrE states when development occurs in the absence of Fgf4 signaling or in presence of a constant high level of exogenous Fgf4 (Nichols et al., 2009; Yamanaka et al., 2010).

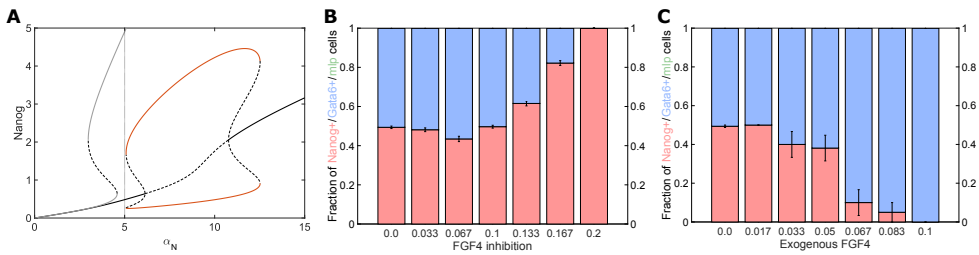

FIGURE 4 Effects of exogenous compounds interfering with the intercellular communication during early development can be predicted by the IHSS (A) Joined bifurcation plot depicting bistable Nanog-Gata behavior on the single-cell level (gray profile) and IHSS on a population level (red), (Eq. (4)). Administering increasing doses of Fgf4 inhibitor (B) or exogenous Fgf4 (C) leads towards increasing occupancies of Epi and PrE fates, respectively.

Considering however that Fgf4 is not a parameter, but rather a variable in the system, we studied the dynamical structure of a minimal model of two coupled cells (Eq. (4)), where the single-cell dynamics is characterized with a bistable behavior (Schröter et al., 2015). Bifurcation analysis demonstrated that not only a co-expression state resembling the ICM emerges due to cell-cell communication, but also a symmetry breaking IHSS occurs, reflecting the differentiation in PrE and Epi fates (Fig. 4A). Numerical simulations of a population of $N = 32$ cells organized at criticality mimicked transitions to either Epi or PrE fates upon signaling perturbations, as experimentally observed (Nichols et al., 2009; Yamanaka et al., 2010). Administering increasing doses of Fgf4 inhibitor effectively diminished the cell-to-cell communication, unravelling single-cell behavior (Nanog state, Fig. 4A, gray profile). Thus, gradual transition towards Epi state was observed (Fig. 4B). On the other hand, increasing the dose of exogenous Fgf4 overwrote the intercellular communication such that the system reflected single cell dose-response behavior, resulting in abrupt switch to high Gata6 expression in the population. The cells thereby either stayed in the salt-and-pepper pattern or transitioned all to the PrE state (Fig. 4C). Taken together, these results suggest that IHSS in conjunction with critical organization, is not only consistent with the existing experimental observations and can explain the robust cell fate specification crucial during early development, but also postulates that increase in cell number through division can provide a reliable timer for differentiation.

3 | DISCUSSION

The emergence of heterogeneous cellular fates characterized with the expression of mutually exclusive expression markers from a multilineage primed state where the different markers are co-expressed, is a long-standing questions that requires both theoretical, as well as experimental attention. The current view is mainly centered on differentiation

being a cell-intrinsic property, where existing asymmetries in the initial expression levels are crucial to drive cells between co-existing attractors (Zhang and Hiiragi, 2018; De Mot et al., 2016; Huang et al., 2007). Although discussed in the context of symmetry breaking, this multistability view formally does not describe such an event, since the stable steady states are already solutions of isolated cells, being populated based on the pre-existing asymmetries. Important insights on a possible symmetry breaking mechanisms in particular during morphogenesis, unquestionably came from Turing's seminal work (Turing, 1952). This formulation however, generally refers to the emergence of spatial organization during development (Turing, 1952; Raspopovic et al., 2014), rather than providing a generic mechanism for differentiation that accounts for reliability and timing of the event. We have proposed here a unique dynamical principle for symmetry breaking on a population level, as a necessary pre-requisite to describe the transition from homogeneous to a heterogeneous distribution of cellular fates during differentiation. We argue that intercellular communication - an integral part of developing embryos, and the respective signaling molecules cannot be treated as parameters in the system, but are rather dynamical variables; thus cells can generate novel dynamical solution when communicating, different from those of the cells in isolation. Both, the multilineage primed- as well as the heterogeneously differentiated states emerge on the level of the population, even when a single steady state characterizes the dynamics of isolated cells. We also propose that fixed organization before the symmetry breaking bifurcation point profiles the number of cells in the population as an effective bifurcation parameter, which combined with the properties of the IHSS solution enables robust cell type ratios to be preserved, as well as provides a possible mechanism for timing. Similar mechanism of a population-based symmetry breaking via a pitchfork bifurcation has been proposed for the Delta-Notch lateral inhibition model, only when the strength of the interaction between the two cells is taken as a bifurcation parameter (Ferrell, 2012). In this case, with organization near criticality the population size can serve as an effective bifurcation parameter if the pitchfork bifurcation is subcritical. Our results therefore demonstrate that symmetry-breaking rather than an asymmetry-based mechanism extensively captures the features of differentiation, especially during early development. In this view, novel information emerges during the symmetry breaking event as pervasive during development, in contrast to the asymmetry-view where the information about cellular types is pre-existing and attractors can be populated at any time point. Thus, viewing differentiation as an emergent computational process rather than unfolding of a pre-determined genetic program allows to propose novel experiments that will further resolve and generalize the self-organization principles in multicellular systems in general.

4 | MATERIALS AND METHODS

4.1 | Generic cell-cell communication system for symmetry breaking

The dynamics of a single cell in the generic model Figs. 1A to 3C is represented with the following set of equations:

$$
\begin{aligned}
\frac{\mathrm{d}u_i}{\mathrm{d}t} &= \lambda(\alpha_u \frac{1}{1+v_i^{\beta}} + \alpha_{u,s} \frac{1}{1+s_{i,ext}^{\eta}} - u_i) \\
\frac{\mathrm{d}v_i}{\mathrm{d}t} &= \lambda(\alpha_v \frac{1}{1+u_i^{\gamma}} - v_i) \\
\frac{\mathrm{d}s_i}{\mathrm{d}t} &= \lambda(\alpha_s \frac{u_i}{1+u_i^{\delta}} - s_i)
\end{aligned}
\tag{1}
$$

Here u and v are the two fate determinant genes that are coupled with mutual inhibition, while s is the secreted

signaling molecule whose production is regulated by u. i - single cell index. In a single cell case, $s_{i,ext} = s_i$, as in Fig. 1A. When intercellular communication is permitted between the cells, the system is distributed spatially on a regular two-dimensional lattice. Three different communication ranges of the secreted signaling molecule, R, were considered: globally connected network (all-to-all communication, $R = \infty$), locally connected network (cells communicate only with direct neighbors on the lattice, $R = 1a$, where a is the lattice constant) and non-locally connected network (cells communicate with direct neighbors and cells on two hops away on the lattice, $R = 2a$). In these cases $s_{i,ext} = \frac{1}{|N_i|+1} \sum_{j \in (N_i \cup i)} s_j$ is the external amount of signal perceived by cell i from its neighborhood N_i, which negatively regulates the production of u. This effectively creates a joint $3N$-dimensional system, where N is the total number of cells (see scheme in Fig. 1B, inset).

$\alpha_{u/v/s/u,s}$ are the production rates, while degradation rates are omitted as the system is globally scaled by λ. β,γ,δ,η are the Hill coefficients. Values of $\alpha_u = 2.3$, $\alpha_v = 3.5$, $\alpha_s = 2$, $\alpha_{u,s} = 1$, $\beta = \gamma = \delta = \eta = 2$, $\lambda = 50$ were used throughout the study.

To discriminate between the multi-lineage-primed- (mlp), u-positive (u+) or v-positive (v+) cell fates for a given realization, each cell vector (u_i,v_i) within the converged state of the system (IHSS or HSS) was individually categorized and the three-term ratios (proportions) were subsequently calculated. Results from 10 repetitions were averaged to generate mean±s.e.m. of the proportions, typically shown on bar diagrams.

For the case of non-identical cells, the α_u parameter was uniformly varied between the cells in the range from −2% to 2% of its value.

For the stochastic simulations a stochastic differential equation model was constructed from Eq. (1) by adding a multiplicative noise term $\sigma X \mathrm{d}W_t$, where $\mathrm{d}W_t$ is the Brownian motion term and X is a variable state. The noise amplitude $\sigma = 0.1$ was used for the cell division case, while $\sigma = 0.5$ was used for the simulations of the Nanog-Gata6 system. The model was solved with $\Delta t = 0.01$ using the Milstein method (Mil'shtein, 1974).

4.2 | Estimating IHSS ditributions as a function of the number of cells (N)

By analogy to Fig. 1E, the different branches of the IHSS (i.e. proportions of cells in them) were estimated using the number of cells as a bifurcation parameter. For this, exhaustive scanning was performed to locate the different fixed point attractors in phase space for each N. The scanning process involved 20 repetitive executions with different noise intensities (varying from 0 to 0.3). Each repetition consisted of 30 alternating cycles of stochastic- (for exploration), followed by deterministic execution (for convergence to attractor) when the reached state was recorded. For every detected attractor the proportion of $u+$ cells was estimated, after which the average u value was calculated and plotted from both, the $u+$ and $v+$ cells, for each such proportion (color-coded, see Fig. 2A).

4.3 | Lineage tree generation

Generation of lineage trees was performed using stochastic simulations where the system doubles in size at regular time intervals, starting from a single cell system to an 8×8-cell system. At every cell division the mother cell's steady state is passes on to daughter cells' initial conditions. Cell divisions occur along horizontal and vertical axis alternately, sequentially yielding lattices of 1×1, 1×2, 2×2, 2×4, 4×4, 4×8 and 8×8. Cellular states were categorized in every time instance to plot the single temporal evolutions in the lineage trees (Figs. 2B and 2C). Further, cellular proportions in the system were estimated from those values and their temporal evolution was shown in the panels above the lineage trees.

In the cell fate sorting case, the steady states of the cells at the end of the fourth cycle were categorized and the differentiated cells were then sorted: $u+$ cells were given as seeds to a new lineage tree, while $v+$ cells were seeds for

a separate one. Following this, multiple cell divisions were again performed and the cell proportions were estimated (Fig. 2C).

4.4 | Multistability model on a single-cell level

Following (Jia et al., 2017) that demonstrated tristability on a single cell level, we introduced cell-cell communication to achieve tristability on a population level (Figs. 3G and 3H) with the following equations:

$$\begin{aligned}\frac{\mathrm{d}A_i}{\mathrm{d}t} &= g_a H^{AA}(A_i, \lambda_{A,A}, n_{A,A}, A_{0,A}) \times H^{BA}(B_i, \lambda_{B,A}, n_{B,A}, B_{0,A}) - k_A A_i + D_A \sum_{j \in N_i} (A_j - A_i) \\ \frac{\mathrm{d}B_i}{\mathrm{d}t} &= g_b H^{BB}(B_i, \lambda_{B,B}, n_{B,B}, B_{0,B}) \times H^{AB}(A_i, \lambda_{A,B}, n_{A,B}, A_{0,B}) - k_B B_i\end{aligned} \tag{2}$$

where the shifted Hill function is used to capture regulation of production of X by Y:

$$H^{YX}(Y, \lambda_{Y,X}, n_{Y,X}, Y_{0,X}) = \frac{1 + \lambda_{Y,X}(\frac{Y}{Y_{0,X}})^{n_{Y,X}}}{1 + (\frac{Y}{Y_{0,X}})^{n_{Y,X}}} \tag{3}$$

Cells communicate via diffusive coupling of A ($D_A = 0.5$). Other parameters: $\lambda_{A,A} = \lambda_{B,B} = 3$, $\lambda_{A,B} = \lambda_{B,A} = 0.1$, $A_{0,A} = B_{0,B} = 80$, $A_{0,B} = B_{0,A} = 20$, $n_{A,A} = n_{B,A} = n_{B,B} = n_{A,B} = 4$, $k_A = k_B = 0.1$, $g_b = 5$. $g_a = 4.035$ was set to place the system in tristability regime.

4.5 | Modeling of the Nanog-Gata6 system

Similarly to the generic u-v symmetry breaking system, the Nanog-Gata6 system was modeled using the following dynamics:

$$\begin{aligned}\frac{\mathrm{d}N(i)}{\mathrm{d}t} &= \lambda(\alpha_N \frac{1}{1 + G(i)^\beta} \frac{1}{1 + (F_{ext}(i) + F_{exo})^\eta} - N) \\ \frac{\mathrm{d}G(i)}{\mathrm{d}t} &= \lambda(\alpha_G \frac{1}{1 + N(i)^\gamma} - G) \\ \frac{\mathrm{d}F(i)}{\mathrm{d}t} &= \lambda(\alpha_F \frac{N(i)}{1 + N(i)^\delta} \frac{1}{1 + (\frac{F_{inh}}{F_{inh,1/2}})^\delta} - F)\end{aligned} \tag{4}$$

Here N, G and F are Nanog, Gata6 and FGF4, respectively. $\alpha_N = 5$ to place the system before the first bifurcation point (Fig. 4A) by analogy to the u-v system, $\alpha_G = \alpha_v$, $\alpha_F = \alpha_s$; $F_{inh,1/2} = 0.1$ for the cases with external inhibition F_{inh} of FGF4 and F_{exo} is the exogenous FGF4 source. The other parameters were as in the u-v system. Locally connected network was used for the corresponding stochastic simulations with multiplicative noise term of 0.5.

The numerical bifurcation analysis was performed using the XPP/AUTO software (Ermentrout, 2016).

All simulation except where explicitly noted were performed using custom-made code in MATLAB (MATLAB and Statistics Toolbox Release R2018b, The MathWorks, Inc., Natick, Massachusetts, United States).

All data and code used in this manuscript are available from the corresponding author upon request.

ACKNOWLEDGEMENTS

The authors thank Philippe Bastiaens for numerous discussions and suggestions that were crucial for the development of this work.

AUTHOR CONTRIBUTIONS

A.K. conceptualized the study, A.S. performed the numerical simulations and bifurcation analysis with help of A.K., and C.S provided valuable insights on the molecular details of early differentiation. A.K. wrote the manuscript with help of A.S. and C.S. All authors read and approved the manuscript.

CONFLICT OF INTEREST

The authors declare that they have no conflict of interest.

REFERENCES

Andrecut, M., Halley, J. D., Winkler, D. A. and Huang, S. (2011) A general model for binary cell fate decision gene circuits with degeneracy: indeterminacy and switch behavior in the absence of cooperativity. *PloS one*, **6**, e19358.

Bessonnard, S., De Mot, L., Gonze, D., Barriol, M., Dennis, C., Goldbeter, A., Dupont, G. and Chazaud, C. (2014) Gata6, Nanog and Erk signaling control cell fate in the inner cell mass through a tristable regulatory network. *Development*, **141**, 3637–3648.

Chazaud, C., Yamanaka, Y., Pawson, T. and Rossant, J. (2006) Early lineage segregation between epiblast and primitive endoderm in mouse blastocysts through the Grb2-MAPK pathway. *Developmental Cell*, **10**, 615–624.

Cherry, J. L. and Adler, F. R. (2000) How to make a biological switch. *Journal of theoretical biology*, **203**, 117–133.

Chickarmane, V. and Peterson, C. (2008) A computational model for understanding stem cell, trophectoderm and endoderm lineage determination. *Plos One*, **3**, e3478.

De Mot, L., Gonze, D., Bessonnard, S., Chazaud, C., Goldbeter, A. and Dupont, G. (2016) Cell fate specification based on tristability in the inner cell mass of mouse blastocysts. *Biophysical Journal*, **110**, 710–722.

Enver, T., Pera, M., Peterson, C. and Andrews, P. W. (2009) Stem cell states, fates, and the rules of attraction. *Cell Stem Cell*, **4**, 387–397.

Ermentrout, B. (2016) XPPAUT. URL: `http://www.math.pitt.edu/~bard/xpp/xpp.html`.

Ferrell, J. E. (2012) Bistability, bifurcations, and Waddington's epigenetic landscape. *Current Biology*, **22**, R458–R466.

Goto, Y. and Kaneko, K. (2013) Minimal model for stem-cell differentiation. *Physical Review E*, **88**.

Graf, T. and Enver, T. (2009) Forcing cells to change lineages. *Nature*, **462**, 587.

Huang, S. (2013) Hybrid T-helper cells: stabilizing the moderate center in a polarized system. *PLoS biology*, **11**, e1001632.

Huang, S., Guo, Y.-P., May, G. and Enver, T. (2007) Bifurcation dynamics in lineage-commitment in bipotent progenitor cells. *Developmental biology*, **305**, 695–713.

Jia, D., Jolly, M. K., Harrison, W., Boareto, M., Ben-Jacob, E. and Levine, H. (2017) Operating principles of tristable circuits regulating cellular differentiation. *Physical biology*, **14**, 035007.

Kauffman, S. A. (1969) Metabolic stability and epigenesis in randomly constructed genetic nets. *Journal of theoretical biology*, **22**, 437–467.

Kauffman, S. A. (1993) *The origins of order: Self-organization and selection in evolution*. OUP USA.

Koseska, A., Ullner, E., Volkov, E., Kurths, J. and Garcia-Ojalvo, J. (2010) Cooperative differentiation through clustering in multicellular populations. *Journal of Theoretical Biology*, **263**, 189–202.

Koseska, A., Volkov, E. and Kurths, J. (2009) Detuning-dependent dominance of oscillation death in globally coupled synthetic genetic oscillators. *Epl*, **85**.

Koseska, A., Volkov, E. and Kurths, J. (2013) Transition from amplitude to oscillation death via Turing bifurcation. *Phys Rev Lett*, **111**, 024103.

Koseska, A., Volkov, E., Zaikin, A. and Kurths, J. (2007) Inherent multistability in arrays of autoinducer coupled genetic oscillators. *Physical Review E*, **75**.

Li, R. and Bowerman, B. (2010) Symmetry breaking in biology. *Cold Spring Harbor perspectives in biology*, **2**, a003475.

Mil'shtein, G. N. (1974) Approximate integration of stochastic differential equations. *Teoriya Veroyatnostei i ee Primeneniya*, **19**, 583–588.

Nichols, J., Silva, J., Roode, M. and Smith, A. (2009) Suppression of Erk signalling promotes ground state pluripotency in the mouse embryo. *Development*, **136**, 3215–3222.

Niwa, H., Toyooka, Y., Shimosato, D., Strumpf, D., Takahashi, K., Yagi, R. and Rossant, J. (2005) Interaction between Oct3/4 and Cdx2 determines trophectoderm differentiation. *Cell*, **123**, 917–929.

Raspopovic, J., Marcon, L., Russo, L. and Sharpe, J. (2014) Digit patterning is controlled by a Bmp-Sox9-Wnt Turing network modulated by morphogen gradients. *Science*, **345**, 566–570.

Saiz, N., Williams, K. M., Seshan, V. E. and Hadjantonakis, A. K. (2016) Asynchronous fate decisions by single cells collectively ensure consistent lineage composition in the mouse blastocyst. *Nature Communications*, **7**.

Schröter, C., Rué, P., Mackenzie, J. P. and Martinez Arias, A. (2015) FGF/MAPK signaling sets the switching threshold of a bistable circuit controlling cell fate decisions in embryonic stem cells. *Development*, **142**, 4205–4216.

Simon, C. S., Hadjantonakis, A.-K. and Schröter, C. (2018) Making lineage decisions with biological noise: Lessons from the early mouse embryo. *Wiley Interdisciplinary Reviews: Developmental Biology*, **7**, e319.

Snoussi, E. H. (1998) Necessary conditions for multistationarity and stable periodicity. *Journal of Biological Systems*, **6**, 3–9.

Suzuki, N., Furusawa, C. and Kaneko, K. (2011) Oscillatory protein expression dynamics endows stem cells with robust differentiation potential. *Plos One*, **6**.

Thomas, R. (1981) On the relation between the logical structure of systems and their ability to generate multiple steady states or sustained oscillations. In *Numerical methods in the study of critical phenomena*, 180–193. Springer.

Turing, A. M. (1952) The chemical basis of morphogenesis. *Philosophical Transactions of the Royal Society of London Series B-Biological Sciences*, **237**, 37–72.

Ullner, E., Koseska, A., Kurths, J., Volkov, E., Kantz, H. and Garcia-Ojalvo, J. (2008) Multistability of synthetic genetic networks with repressive cell-to-cell communication. *Physical Review E*, **78**.

Wang, J., Zhang, K., Xu, L. and Wang, E. (2011) Quantifying the Waddington landscape and biological paths for development and differentiation. *Proceedings of the National Academy of Sciences*, **108**, 8257–8262.

Yamanaka, Y., Lanner, F. and Rossant, J. (2010) FGF signal-dependent segregation of primitive endoderm and epiblast in the mouse blastocyst. *Development*, **137**, 715–724.

Zhang, H. T. and Hiiragi, T. (2018) Symmetry breaking in the mammalian embryo. *Annual review of cell and developmental biology*, **34**, 405–426.